11th World Congress on Computational Mechanics (WCCM XI)
5th European Conference on Computational Mechanics (ECCM V)
6th European Conference on Computational Fluid Dynamics (ECFD VI)
E. Oñate, J. Oliver and A. Huerta (Eds)

SIMULATION OF CYCLIC OEDOMETRIC COMPRESSION TEST WITH THE MATERIAL POINT METHOD AND THE SUBLOADING CAM CLAY MODEL

RAYDEL LORENZO[*], MANOEL P. CORDÃO NETO[†] AND RENATO P. DA CUNHA[†]

[*] PhD. student at Geotechnical Post-Graduation program at University of Brasilia
Campus Darcy Ribeiro, SG12 Brasilia, Brazil.
rlorenzo@unb.br, www.geotecnia.unb.br/gpfees

[†] Professor at Geotechnical Post-Graduation Program at University of Brasilia
mporfirio@gmail.com, www.geotecnia.unb.br

Professor at Geotechnical Post-Graduation Program at University of Brasilia
rpcunha@gmail.com, www.geotecnia.unb.br/gpfees

Key Words: *Material Point Method, Cyclic loading, Subloading Model, Cam Clay Model.*

Abstract. The Material Point Method (MPM) has gained space in dynamics problems. In geotechnical engineering this problems appear in areas like foundations of machines, earthquakes, wave attack, construction of sand compaction piles and others. In dynamical simulations is very common to occur loading and unloading paths. Proper constitutive models have to be used to consider the irreversible deformations that can appear in cyclic loading. In this paper, the SubCam model is implemented in a code of MPM. This model introduces the concept of subloading surface to the well-known Modified Cam Clay model (MCC). Consequently, a smooth transition between the elastic and elasto-plastic behaviour of the soil is obtained. Moreover, plastic strains are developed inside the yield surface, as it is observed in real tests. The model introduces only one more parameter than the MCC. Therefore, more realistic results can be obtained with little increment of effort. The fundamental discrepancies in the implementation of the model compared to the MCC are also presented in this paper. The SubCam model can better reproduce the behaviour of the soil and it's easier to implement. Cyclic isotropic and oedometric compression tests are simulated as benchmarks to evaluate the implementation of the model. Also, the response of the model to different values of the new parameter is evaluated.

1 INTRODUCTION

In the last years the finite element method (FEM) has become the standard tool for solve the majority of the analysis in solid mechanics. Nevertheless, this method, in his traditional

Lagrangian formulation is not suitable for the analysis of large deformation [1], [2].

According to [3] when this type of problems is simulated with this formulation, great distortions of the mesh can occur and remesh can be needed. During the process of remesh all the state variables need to be mapped from the distorted mesh to the new one. This can lead to the introduction of numerical errors in the calculation.

To solve the difficulties with FEM in the simulation of large deformation problems mesh less methods has been developed. For these the generation of the mathematical problems reduces to the generation of material points and his distribution, without fix connectivity between them, as in FEM. Some of these methods are the discrete element method (DEM), smooth particle hydrodynamics (SPH) and particle in cell method (PIC) [4]. Each of these methods has advantage and disadvantage in the simulation of solid mechanics with large deformation. Some associated with the properties or characterization of the material as in DEM other with delineating material boundaries as in PIC.

The Material Point Method is a type of PIC [5]. This combines ideas and procedures of the particle methods and the finite element method. It uses the potential of the Lagrangian and Eulerian descriptions of kinematics. With MPM a body is modelled as a group of Lagrangian particles. This particles transport the state variables and other variables needed to solve the kinematics equations. These variables are interpolated from particles to a fixed mesh in which the equations of motion are solved. After have obtained the solution it is interpolated to the particles and the state variables and positions are updated. This procedure is repeated for all the time domain of the problem. In this way the fixed mesh have no distortion [6].

In the last decade a generalization to MPM was done to eliminate numerical noise that arises when a particle crosses from one cell to another. This method is known as Generalized Interpolation Material Point (GIMP) and was introduced by [6]. New interpolation functions were introduced with a domain bigger than a cell, allowing tracking a particle when go out of his original cell. More recently, a modification was introduced to the GIMP method to solve problems that appears when large distortions and tensions occur. This new methods is known as Convected Particle Domain Interpolation (CPDI) as it was presented by [7].

The numerical code used was developed by [8] an is called *NairnMPM.* This code allows doing 2D and 3D dynamic analysis and in the present version allows to use GIMP and CPDI.

In a previous paper, the authors presented the implementation and validation of the Modified Cam Clay model (MCC) in a code based in MPM [9]. Herein, a model that improves the results of the simulations especially to cyclic loading is implemented and validated in a MPM code. This constitutive model is known as Subloading Cam Clay (SubCam) and was presented by [10]. Details of the implementation, and certifications results derived from comparison with tri-axial and oedometric cyclic test are presented and discussed.

2 BRIEF DESCRIPTION OF MPM

The MPM use a mixed description between Lagrangian and Eulerian. The method was developed from a method known as Fluid Implicit Particle (FLIP) that was first applied to fluid problems [11] been the MPM an extension to the case of solid mechanics [12]. The method was presented in terms of the FEM by [5], [13] to allow a more easy understanding.

With MPM a body is modeled by a group of non-connected particles. The particles transport the mass and all the properties that are necessary to define the complete problem. The variables are interpolated from the particles to the nodes of a fixed mesh where the equations of the problem are solved. After that the results are return interpolated to the particles and the state variables are updated. This procedure is repeated for the time steps until the complete time of simulation is reached.

The MPM is suitable for dynamic problems with large deformations, impact problems and contact and penetration between bodies [14], [15].

A complete algorithm of the MPM for solving mechanics problems is presented in Figure 1. This algorithm is for the case where the constitutive law is integrated before solve the momentum conservation equation. This case is called update strain first (USF). Another two ways are used depending on the time moment where the integration is done. These are known as update strain last (USL) and update strain average (USAVG). This last one use the other two methods and give as result for the time step the average of the obtained values [16]. The difference in the solutions using these methods is related to the energy point of view. In [17] attention is focused in the numerical characteristics of these methods. It is found that the USF approach gives a better conservation of the energy than the USL approach.

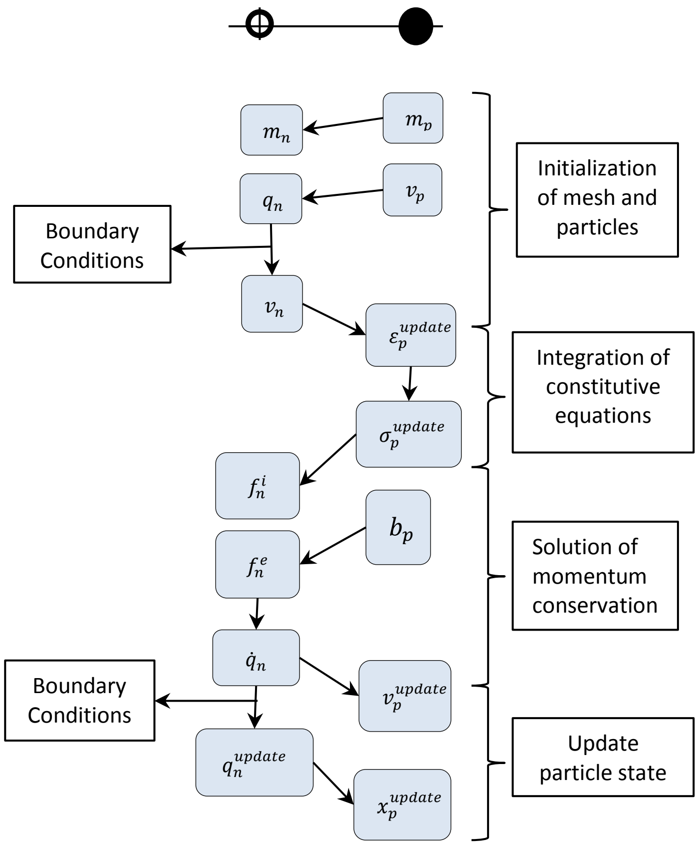

1- Calculate m_n from m_p

2- Calculate $\underset{\sim}{q}_n$ from m_p and $\underset{\sim}{v}_p$

3- Calculate $\underset{\sim}{v}_n$ from de $\underset{\sim}{q}_n$ and m_n

4- Calculate $\underset{\approx}{\varepsilon}_p$ from $\underset{\sim}{v}_n$

5- Update $\underset{\approx}{\sigma}_p$ from $\underset{\approx}{\varepsilon}_p$

6- Calculate $\underset{\sim}{f}_n^{\text{int}}$ from $\underset{\approx}{\sigma}_p$

7- Calculate $\underset{\sim}{f}_n^{ext}$ from $\underset{\sim}{b}$ and $\underset{\sim}{t}$

8- Calculate $\dot{\underset{\sim}{q}}_n$ from $\underset{\sim}{f}_n^{\text{int}}$ and $\underset{\sim}{f}_n^{ext}$

9-Update $\underset{\sim}{x}_p$ and $\underset{\sim}{v}_p$

Figure 1: Calculation algorithm for the MPM and variables calculated in the node and the particles [modified of 17].

The formulation of the method applied to kinematic problems can be found in elsewhere [16], where particular details of the implementations are presented in [17].

3 SUBLOADING CAM CLAY MODEL

The elasto-plastic theory is nowdays the largest source of constitutive models applied to geomechanics [18]. The great contribution of the geotechnics to the constitutive models is the framework of the critical state theory presented by [19]. One of the most used models based on these theories is the Modified Cam Clay (MCC). This model is relatively simple and captures the features of the behavior of normally consolidated clays in a good manner. Nevertheless, this model has problems describing some important features of soil behavior, such as, positive dilatancy during strain hardening, cyclic loading, influence of density and/or confining pressure on deformation and strength.

In his original form, the MCC give for overconsolidated clays a non-linear elastic behavior under unloading and reloading. However, real clays show elastoplastic behavior even in the overconsolidation region [20]. To solve this problems was introduced by [21] the subloading surface concept. This surface is internal to the yield surface and has the same geometry form. In the stress space, the actual stress point is always on the Subloading surface and the evolution of the surface is dependent of the elastoplastic transition. The models introduced with this concept were known as surface loading models [22].

The incorporation of the subloading concept to a model, increase an internal variable. This variable defines the size of the subloading surface and it is a measure of the densification in the case of sands or the overconsolidation in the case of clays (see Figure 2). The introduction of this variable to a conventional elastoplastic model, improves the capacity of the model in reproduce the cyclic behavior [20].

The SubCam model proposed by [10] introduce the subloading surface to the well-known MCC. This model considers the influence of density and confining pressure on the deformation and strength of soils [23]. The SubCam model has been used in finite elements codes with success [24], [25].

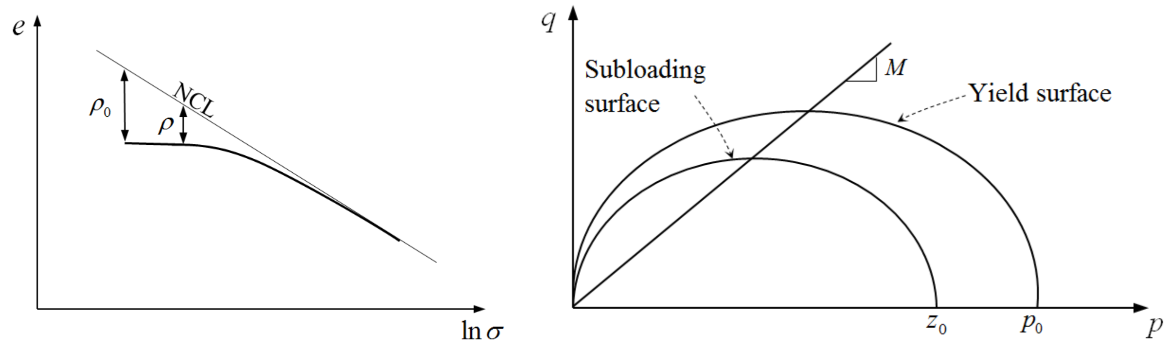

Figure 2: Void ratio - $\ln\sigma$ relation in overconsolidated clay [20].

3.1 Brief Description of Modified Cam Clay model.

The MCC model was developed for triaxial conditions. This model was introduced by [19] and represents a slight extension of Cam Clay model by adopting a revised work equation to derive the yield function and plastic potential.

The yield surface of the model is defined in the mean effective stress (p') - deviatoric stress (q) plane as forming an ellipse.

$$f = M^2\left(p^2 - p_0 p'\right) + q^2 \tag{1}$$

Where M is the slope of the critical state line and p_0 is the pre-consolidation stress. Hardening is defined as a function of the plastic volume deformation (ε_v^p) in the following form:

$$\frac{dp_0}{p_0} = \frac{(\lambda - \kappa)}{(1+e)}\varepsilon_v^p \tag{2}$$

Where λ is the slope of the normal compression line in the space of $\ln p'$ versus the void ratio (e) and κ is the slope of the unloading-reloading line in the same space. It is assumed an associated flow rule, i.e. $f(\sigma, p_0) = g(\sigma, p_0)$, where $g(\sigma, p_0)$ is the plastic flow function and σ the Cauchy stress tensor. The flow rule and the plastic multiplier are represented as:

$$d\underset{\approx}{\varepsilon}^p = \lambda_p \frac{\partial g}{\partial \underset{\approx}{\sigma}} \tag{3}$$

$$\lambda_p = \frac{\dfrac{\partial f}{\partial \underset{\approx}{\sigma}}^T : \underset{\approx}{D}^e : d\underset{\approx}{\varepsilon}}{\dfrac{\partial f}{\partial \underset{\approx}{\sigma}}^T : \underset{\approx}{D}^e : \dfrac{\partial g}{\partial \underset{\approx}{\sigma}}^T - \dfrac{\partial f}{\partial \varepsilon_v^p} tr\left(\dfrac{\partial f}{\partial \underset{\approx}{\sigma}}\right)} \tag{4}$$

Where $tr(\ )$ represent the trace of the entity and D^e the elastic constitutive tensor.

In this model, as in the models based in the general elastoplastic theory, after the integration of the constitutive equation, it is necessary to verified if the predicted stresses satisfy the consistency condition. Even using small steps, in the post yield range, it is found in practice that the predicted state of stress at the end of a loading increment may not lead to the correct yield surface. Given such feature it is necessary to introduce a method for projecting back the state of stress to the yield surface [26].

3.2 SubCam math definitions

The SubCam model defines the new variable ρ. This variable is a measure of the density or the overconsolidation of the soil and becomes null when the stress path reaches the normal compression line (NCL). It is related to the overconsolidation ratio as:

$$\rho = (\lambda - \kappa)\ln\left(\frac{p_0}{z_0}\right) \tag{5}$$

where z_0 is the interception of the subloading surface with the isotropic compression axis. The same flow rule defined for the yield surface in the MCC is used in the SubCam. For the subloading surface, another flow rule is defined wish considers a strain variable known as subloading plastic strain ($\varepsilon_v^{p(SL)}$).

$$dz_0 = \frac{z_0\left(1+e_0\right)}{\left(\lambda-\kappa\right)}\left(d\varepsilon_v^p + d\varepsilon_v^{p(SL)}\right) \tag{6}$$

According to [27], $\varepsilon_v^{p(SL)}$ can be obtained as:

$$\varepsilon_v^{p(SL)} = \frac{-\rho}{\left(1+e_0\right)} = \lambda_p \frac{G\left(\rho\right)}{p} \tag{7}$$

Where $G\left(\rho\right)$ is a function that controls the degradation of ρ. This function was proposed by [27] as $G\left(\rho\right) = a\rho^2$. The parameter (a) is the only new parameter added by this model to the MCC model and would be obtained by calibration of the model with oedometric tests.

Considering the consistency condition and $\varepsilon_v^{p(SL)}$ the plastic multiplier can be obtained as:

$$\lambda_p^{SL} = \frac{\dfrac{\partial f}{\partial \underset{\approx}{\sigma}}^T : \underset{\approx}{D}^e : d\underset{\approx}{\varepsilon}}{\dfrac{\partial f}{\partial \underset{\approx}{\sigma}}^T : \underset{\approx}{D}^e : \dfrac{\partial g}{\partial \underset{\approx}{\sigma}}^T - \dfrac{\partial f}{\partial z_0}\dfrac{z_0\left(1+e_0\right)}{\left(\lambda-\kappa\right)}\left(tr\left(\dfrac{\partial f}{\partial \underset{\approx}{\sigma}}\right)+L\right)} \tag{8}$$

$$L = a\frac{\left(\dfrac{\left(\lambda-\kappa\right)}{\left(1+e_0\right)}\ln\left(\dfrac{p_0}{z_0}\right)\right)^2}{p} \tag{9}$$

Where L is an auxiliary function.

The consistency condition in this case is applied to the subloading surface and not to the yield surface as in normal elasto-plastic models.

If the derivative related to the internal variables are replaced in expressions (4) and (8) the plastic multiplier are expressed as:

$$\lambda_p = \frac{\dfrac{\partial f}{\partial \underset{\approx}{\sigma}}^T : \underset{\approx}{D}^e : d\underset{\approx}{\varepsilon}}{\dfrac{\partial f}{\partial \underset{\approx}{\sigma}}^T : \underset{\approx}{D}^e : \dfrac{\partial g}{\partial \underset{\approx}{\sigma}}^T + \left(M^2 p \dfrac{p_0\left(1+e_0\right)}{\left(\lambda-\kappa\right)}\right) tr\left(\dfrac{\partial f}{\partial \underset{\approx}{\sigma}}\right)} \tag{10}$$

$$\lambda_p^{SL} = \frac{\dfrac{\partial f}{\partial \underset{\approx}{\sigma}}^T : \underset{\approx}{D}^e : d\underset{\approx}{\varepsilon}}{\dfrac{\partial f}{\partial \underset{\approx}{\sigma}}^T : \underset{\approx}{D}^e : \dfrac{\partial g}{\partial \underset{\approx}{\sigma}}^T + \left(M^2 p \dfrac{z_0\left(1+e_0\right)}{\left(\lambda-\kappa\right)}\right)\left(tr\left(\dfrac{\partial f}{\partial \underset{\approx}{\sigma}}\right)+L\right)} \tag{11}$$

As can be seen in equations (10) and (11), the only difference between the equations is the function L. When the subloading surface reaches the yield surface the value of L becomes zero and the SubCam behaves as the MCC.

When the parameter a is very small then the plastic multiplier will be very large and plastic strains will appear since the beginning of the loading.

4 VALIDATION OF THE IMPLEMENTED SUBCAM MODEL

As stated before, the SubCam model was implemented in a code of GIMP, called *NairnMPM* code. This code was developed by Professor John Nairn at the University of Oregon. The code is explicit and allows 2D and 3D numerical analyses. It was written in C++ and incorporates distinct material models, especially those related to mechanical and wood engineering. More details about the *NairnMPM* can be found in [8].

In a previous work the authors presented the results of the implementation of the MCC in the *NairnMPM.* This implementation allows the incorporation of earth-like materials in an easy way [9]. Herein the SubCam model is implemented and validated. Simulations with known stress path were conducted to test the model.

Figure 3 shows simulated isotropic compression paths with the same parameters but with different values of a.

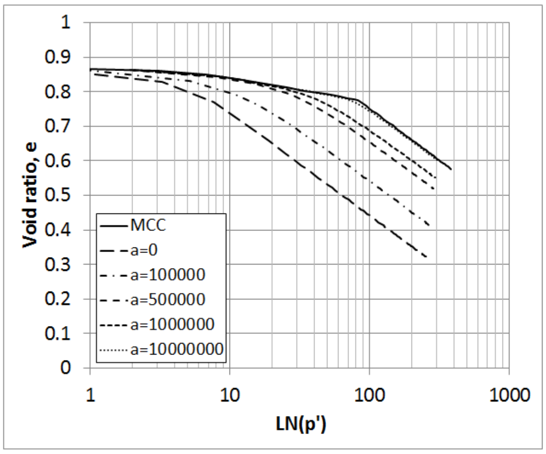

Figure 3: Isotropic compression paths for different values of the subloading parameter (a)

It can be observed as with a value of $a = 10000000$ the result of the SubCam model is almost the same of the MCC. The only difference is that the SubCam has a smooth transition from elastic to elasto-plastic behavior. This smooth transition improves the results obtained by this model when used in boundary conditions problems. Furthermore, the adjustment of the type of curve obtained by the SubCam is better when compared with real isotropic and oedometer compression tests.

Conventional triaxial compression tests (CTC) were simulated. Figure 4 presents the stress and strain path for one material point of the virtual sample. The non-normal curvature in the *p*-*q* plane near the critical state line (CSL) is because the applications of the loads were done in the surfaces of the sample. These surfaces near the rupture are non-longer parallel and the simulation test continuous with a different path of a CTC test.

Another CTC test was done to show the response of the model to trajectories in the dry side (OCR>2). The softening response in these trajectories using the MCC model is only achieved when used a return algorithm. As can be seen in Figure 5, although the MCC model captures the softening feature of the soil, a peak appears at the maximum value of the deviatoric stress. This peak does not appear in real soil behavior.

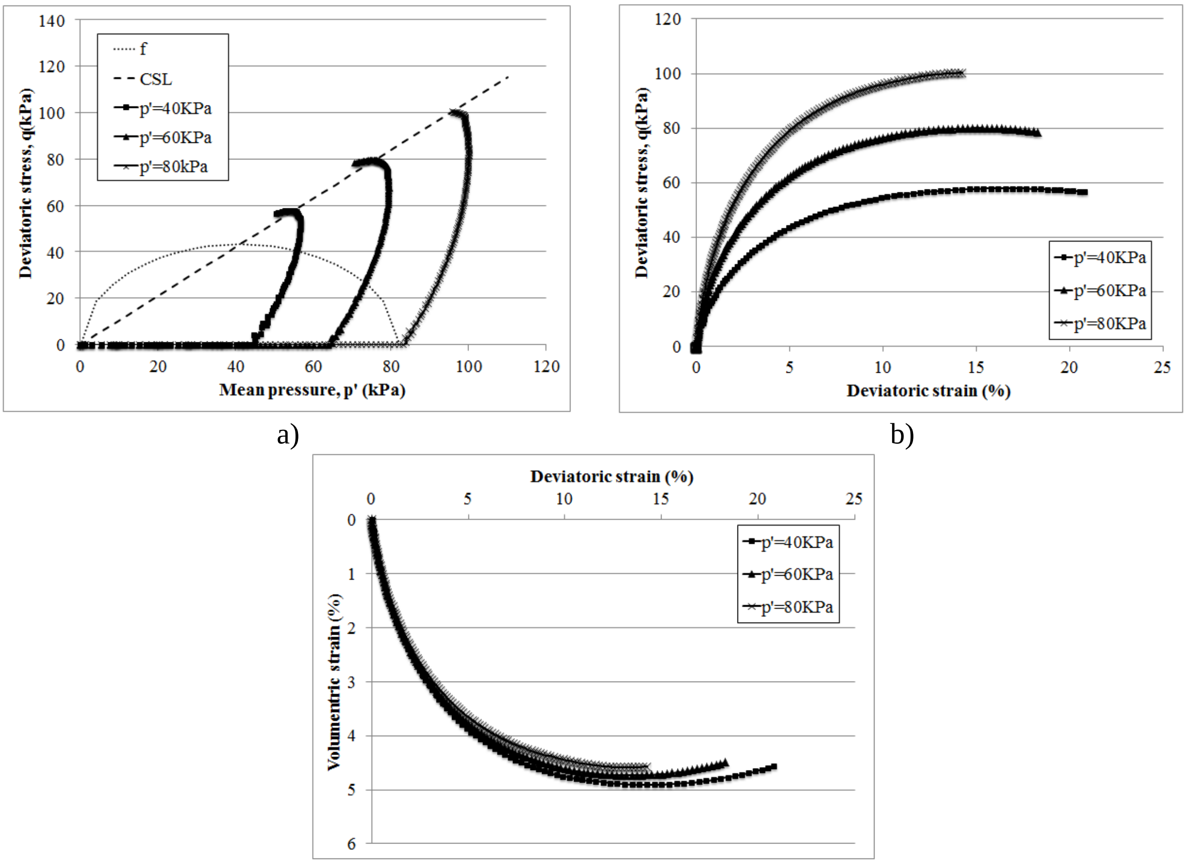

a) b)

c)

Figure 4: Conventional tri-axial compression test simulation results for one material point, with $a = 100000$.

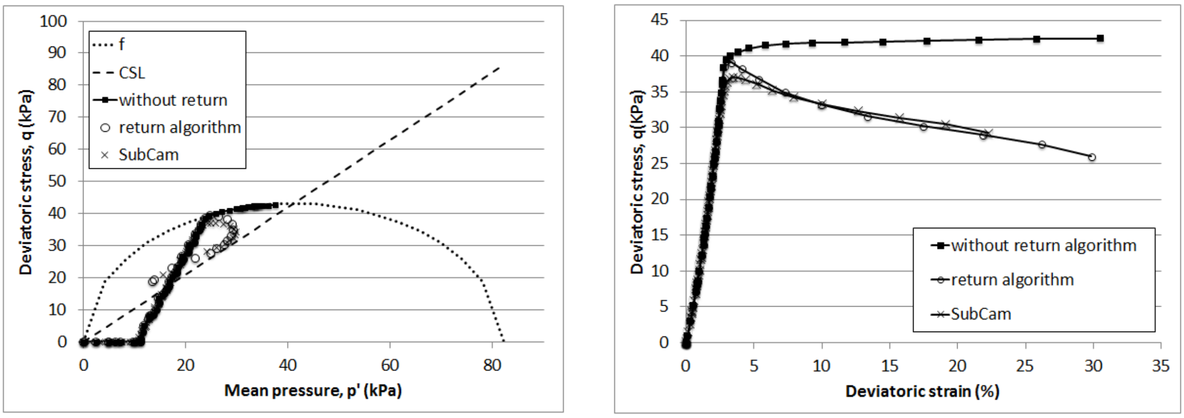

a) b)

Figure 5: Conventional tri-axial test in the dry side for the MCC (with and without return algorithm) and the SubCam model.

As can be seen in Figure 5, the SubCam model improves these results. Therefore, the introduction of the subloading concept and the variable ρ to the MCC model, improves the response of the simulations in case of overconsolidated clays and dense sands.

4.1 Cyclic Oedometer test

Cyclic loading appears in various geotechnical engineering cases. The evaluations of the serviceability limits in these cases are a key point. Some examples of cyclic loading appear in offshore foundations, railways lines, wind turbines foundations and others.

The soil response to cyclic loading conditions is more difficult to be simulated. This is partly because of the hysteresis behavior. The use of appropriated constitutive models in the simulations of this type of loading is essential. Figure 6 shows the results of two oedometer compression test simulations, one using the MCC model and the other the SubCam model.

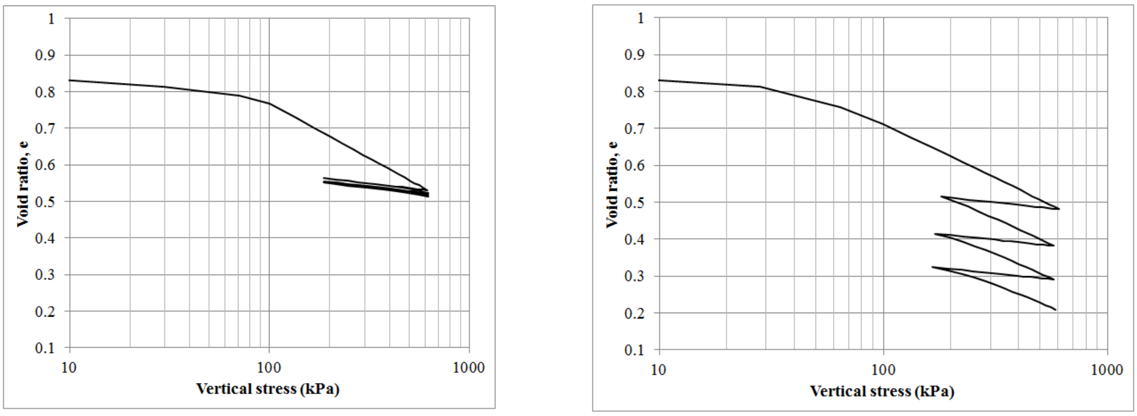

a) b)

Figure 6: Cyclic oedometer compression test simulation. a) MCC b) SubCam

As can be seen in the simulation with the MCC model, during the cyclic loading no deformations occur. In real soils behavior, something more like the curve obtained using the SubCam model is expected. It is worst to note that with the SubCam model the deformations increase in each cycle tend to decrease. This phenomenon is also observed in real soils behavior where with a large number of cycles the deformations tend to stabilize.

5 CONCLUSIONS

- The SubCam model can be implemented with a little effort once the MCC model has already been implemented.
- The behavior of dense sands and overconsolidated clays is reproduced better by the Subloading Cam Clay model than the Modified Cam Clay model.
- The cyclic oedometric compression test behavior of the soil was simulated with the SubCam model and the results reproduced better the response of the soil.

REFERENCES

[1] S. G. Bardenhagen, J. U. Brackbill, and D. Sulsky, “The material-point method for granular materials,” *Comput. Methods Appl. Mech. Eng.*, vol. 187, no. 3–4, pp. 529–541, Jul. 2000.

[2] Z. Wieckowski, “The material point method in large strain engineering problems,” *Comput. Methods Appl. Mech. Eng.*, vol. 193, no. 39–41, pp. 4417–4438, Oct. 2004.

[3] L. Beuth, T. Benz, and P. A. Vermeer, “Large deformation analysis using a quasi-static Material Point Method,” in *Computer Methods in Mechanics*, 2007, pp. 1–6.

[4] F. Zabala, “Modelación de problemas geotécnicos hidromecánicos utilizando el método del punto material,” Universidad Politécnica de Catalunya, 2010.

[5] D. Sulsky, Z. Chen, and H. L. Schreyerb, “A Particle Method for History-Dependent Materials,” *Comput. Methods Appl. Mech. Eng.*, vol. 118, no. 1, pp. 179–196, 1994.

[6] S. G. Bardenhagen and E. M. Kober, “The Generalized Interpolation Material Point Method,” *Tech Sci. Press*, vol. 5, no. 6, pp. 477–495, 2004.

[7] A. Sadeghirad, R. M. Brannon, and J. Burghardt, “A convected particle domain interpolation technique to extend applicability of the material point method for problems involving massive deformations,” *Int. J. Numer. Methods Eng.*, vol. 86, no. 12, pp. 1435–1456, 2011.

[8] J. Nairn, “Source code and documentation for NairnMPM Code for Material Point Calculations. http://oregonstate. edu/~nairnj/.” 2011.

[9] R. Lorenzo, R. P. Cunha, and M. P. Cordão Neto, “Materal point method for geotechnical problems involving large deformation,” in *III International Conference in Particles-Based Methods*, 2013, p. 12.

[10] D. M. Pedroso, “Representação Matemática do Comportamento Mecânico Cíclico de Solos Saturados e Não Saturados,” Universidade de Brasília, 2006.

[11] Harlow F. H., “The Particle-In-Cell computing method in fluid dynamics,” *Methods Comput. Phys.*, vol. 3, pp. 319–343, 1964.

[12] C. J. Coetzee, “The Modelling of Granular Flow Using the Particle-in-Cell Method,” PhD. Thesis, University of Stellenbosch, 2004.

[13] D. Sulsky and H. L. Schreyerb, “Axisymmetric form of the material point method with applications to upsetting and Taylor impact problems,” *Comput. Methods Appl. Mech. Eng.*, vol. 139, pp. 409–429, 1996.

[14] H. W. Zhang, K. P. Wang, and Z. Chen, “Material point method for dynamic analysis of saturated porous media under external contact/impact of solid bodies,” *Comput. Methods Appl. Mech. Eng.*, vol. 198, no. 17–20, pp. 1456–1472, Apr. 2009.

[15] S. G. Bardenhagen, J. Nairn, and H. Lu, “Simulation of dynamic fracture with the Material Point Method using a mixed J-integral and cohesive law approach,” *Int. J. Fract.*, vol. 170, no. 1, pp. 49–66, Jun. 2011.

[16] J. Nairn, “Material Point Method Calculations with Explicit Cracks,” *Comput. Model. Eng. Sci.*, vol. 4, no. 6, pp. 649–663, 2003.

[17] O. Buzzi, D. M. Pedroso, and A. Giacomini, “Caveats on the Implementation of the Generalized Material Point Method,” *Tech Sci. Press*, vol. 31, no. 2, pp. 85–106, 2008.

[18] L. Zdravkovic and J. P. Carter, "Contributions to Géotechnique 1948–2008: Constitutive and numerical modelling," *Géotechnique*, vol. 58, no. 5, pp. 405–412, Jan. 2008.
[19] Roscoe and Burland, "On the generalised stress-strain behaviour of 'wet clay,'" *Eng. Plast.*, pp. 535–609, 1968.
[20] T. Nakai, *Constitutive Modeling of Geomaterials*, Taylor & F. Boca Raton: CRC Press, 2013, p. 360.
[21] K. Hashiguchi and M. Ueno, "Elastoplastic Constitutive laws of soils," in *9th ICSMFE Special Session 9*, 1977, pp. 73–82.
[22] M. Hira, K. Hashiguchi, M. Ueno, and T. Okayasu, "DEFORMATION BEHAVIOR OF SHIRASU SOIL BY YHE EXTENDED SUBLOADING SURFACE MODEL," *Lowl. Technol. Int.*, vol. 8, no. 1, pp. 37–46, 2006.
[23] M. M. Farias, D. M. Pedroso, and T. Nakai, "Automatic substepping integration of the subloading tij model with stress path dependent hardening," *Comput. Geotech.*, vol. 36, no. 4, pp. 537–548, May 2009.
[24] M. M. Farias, T. Nakai, H. M. Shahin, D. M. Pedroso, P. G. O. Passos, and M. Hinokio, "Ground Densification due to sand compaction piles," *Soils Found.*, vol. 45, no. 2, pp. 167–180, 2005.
[25] H. D. Gallego-Herrera, "Análise do Comportamento de Rejeito de Mineração Durante a Construção de um Aterro Experimental," Departamento de Engenharia Civil e Ambiental, Universidade de Brasília, 2012.
[26] D. M. Potts and A. Gens, "A critical assessment of methods of correcting for drift from the yield surface in elasto-plastic finite element analysis," *Int. J. Numer. Anal. Methods Geomech.*, vol. 9, pp. 149–159, 1985.
[27] T. Nakai and M. Hinokio, "A simple elastoplastic model for normally and over consolidated soils with unified material parameters," *Soils Found.*, vol. 44, no. 2, pp. 53–70, 2004.